

Spin waves modulated in a ferromagnetic bilayer system calculated using the interface rescaling approach

Wen Ping Zhou,^{1,3,*} Guo Hong Yun,^{1,2,3} and Xi Xia Liang^{1,3}

¹Laboratory of solid State Physics, Department of Physics, Inner Mongolia University, Inner Mongolia, Hohhot 010021, People's Republic of China

²Department of Physics, Inner Mongolia Normal University, Inner Mongolia, Hohhot 010021, People's Republic of China

³CCAST (World Laboratory), P.O. Box 8730, Beijing 100080, People's Republic of China

(Received 19 December 2006; revised manuscript received 5 December 2007; published 5 March 2008)

The eigenproblems of spin waves in a ferromagnetic bilayer system with periodic boundary conditions are solved using the interface-rescaling approach. The Brillouin zone mapping of the system is investigated. Besides three types of known eigenmodes, the bulk mode, the interface mode, and the perfect confined mode, we also find a type of eigenmode, the critical mode, on the boundary of those known eigenmodes, which is composed of the spin wave modulated. This spin wave possesses both the feature of the bulk spin wave and that of the interface spin wave.

DOI: 10.1103/PhysRevB.77.104403

PACS number(s): 75.30.Ds

I. INTRODUCTION

The giant magnetoresistance effect was found in magnetic multilayers more than ten years ago.¹ Since then, magnetic multilayers have been the key configurations in the field of the condensed matter physics research² boosted by their potential application in the magnetic field sensors,³ the spin valve read head for hard drives,⁴ the magnetoresistive random access memory,⁵⁻⁸ and so on. At the same time, rapid increase of processor speeds in modern computers leads to the necessity to write bits of information during nanosecond time intervals,⁹ while this time scale is determined by the eigenfrequencies of the layered recording media. So the experimental¹⁰⁻¹⁵ and theoretical¹⁶⁻²⁷ studies of the eigenexcitations in the magnetic multilayered systems are of great importance. In all the studies, only the diagrammatic sketch of the energy band is given and three kinds of spin waves are found, the bulk mode (BM), the interface mode (IM), and the perfect confined mode (PCM). However, we first give the fine structure of the energy band of the Brillouin zone and also find a kind of mode, namely, the critical mode (CM), in the ferromagnetic bilayered systems, which may exist at the critical position between BM and PCM or PCM and IM. CM is composed of the spin waves modulated by the interface (SWM), which possess both the feature of the bulk spin waves and that of the interface spin waves.

This paper is organized as follows. Section II introduces the model and gives the classification of spin eigenmodes. In Sec. III, we give the energy band fine structure and discuss the critical mode. In Sec. IV, conclusions are drawn.

II. MODEL AND EIGENMODES

We consider a simple cubic ferromagnetic bilayer slab consisting of two different sublayers *A* and *B* with the bulk-exchange interactions J_A and J_B , the interface exchange coupling J_{AB} , the spins S_A and S_B , and the numbers of lattice planes N_A and N_B , respectively. For the sake of simplicity, we assume the two ferromagnets still have their periodicity in the lattice planes parallel to the interface. Here, we neglect

the anisotropy in the bulk, on the interface, and on the surfaces, so that the inhomogeneity of the system is assumed to come from the difference between the interface and bulk-exchange couplings J_{AB} , J_A , and J_B . Under a periodic boundary condition, we assume the Heisenberg Hamiltonian consists of a term accounting for the isotropic nearest-neighbor exchange interaction. Hence, the Hamiltonian of such system is written as

$$\hat{H} = - \sum_{n,m} \sum_{i,j} J(n,i;m,j) \mathbf{S}(n,i) \cdot \mathbf{S}(m,j), \quad (1)$$

where $N_A + N_B = N$, and n, m are the indices of the lattice planes and i, j are the sites in the atomic planes n and m , respectively. The interaction constant $J(n,i;m,j)$ takes, respectively, J_A for both sites in sublayer *A*, J_B for both sites in sublayer *B*, J_{AB} for one site in sublayer *A* and the other in sublayer *B*. The spin operators satisfy the following equation:

$$\begin{aligned} \hat{S}(n,i) \cdot \hat{S}(n,i) &= S(n)[S(n) + 1] \\ &= \begin{cases} S_A(S_A + 1) & \text{for sites in } A \\ S_B(S_B + 1) & \text{for sites in } B. \end{cases} \end{aligned} \quad (2)$$

Using the interface-rescaling approach,¹⁹ the Hamiltonian can be easily diagonalized and the eigenequations of the spin waves of the system can be obtained as follows:

$$\begin{aligned} E_{pk} f(n,p) &= [J(n,n)S(n) + J(n,n+1)S(n+1) \\ &\quad + J(n,n-1)S(n-1)]f(n,k) \\ &\quad - J(n,n+1)\sqrt{S(n)S(n+1)}f(n+1,k) \\ &\quad - J(n,n-1)\sqrt{S(n)S(n-1)}f(n-1,k), \end{aligned} \quad (3)$$

where

$$J(n,n) = 2(2 - \cos k_x - \cos k_y)J(n,i;n,i \pm 1) \equiv 2\gamma J_n,$$

$$J(n, n \pm 1) = J(n, i; n \pm 1, i) = J(n \pm 1, n). \quad (4)$$

Here, E_{pk} (>0) is the excitation energy of the spin waves and $f(n, p)$ is an orthonormalized wave function, which satisfies Born-Karman boundary condition. The index p in the wave functions is the wave vector of the spin waves parallel to the interface, and the parameter $\gamma = \gamma(k_{\parallel}) = \gamma(k_x, k_y)$ defined by Eq. (4) varies from 0 to 4. We have chosen the lattice constants in both sublayers as unit length, i.e., the excitation energy and the wave vector of the spin waves mentioned in this paper are, respectively, the reduced excitation energy and the reduced wave vector.

Considering the periodic boundary condition, we assume the interfaces are formed between the planes $n=1, N$ and $n=N_A, N_A+1$ for the present slabs. We will neglect the indices p, k of E_{pk} and p of $f(n, p)$ for simplicity and set

$$f(n) = \begin{cases} f_A(n) & \text{for } 1 \leq n \leq N_A \\ f_B(n) & \text{for } N_A + 1 \leq n \leq N. \end{cases} \quad (5)$$

Due to the periodic boundary condition and the inversion symmetry in this system, the wave function $f(n)$ in the two sublayers may be written, respectively, as

$$f_A(n) = \begin{cases} D_A^C \cos\{k_A[n - \frac{1}{2}(N_A + 1)]\}, & P = +1 \\ D_A^S \sin\{k_A[n - \frac{1}{2}(N_A + 1)]\}, & P = -1, \end{cases} \quad (6a)$$

$$f_B(n) = \begin{cases} D_B^C \cos\{k_B[n - N_A - \frac{1}{2}(N_B + 1)]\}, & P = +1 \\ D_B^S \sin\{k_B[n - N_A - \frac{1}{2}(N_B + 1)]\}, & P = -1, \end{cases} \quad (6b)$$

where D_i^j ($i=A, B; j=C, S$) is a normalization constant, P represents the even parity ($P=+1$) or the odd parity ($P=-1$), and k_A and k_B are, respectively, the wave-vector components perpendicular to the interfaces between sublayers A and B .

We define the interface-rescaling coefficient R as follows:²⁰

$$\begin{aligned} f_B(N) &= Rf_A(1), \\ f_B(N_A + 1) &= Rf_A(N_A). \end{aligned} \quad (7)$$

Inserting R into Eq. (3) and using the periodic boundary condition, one can obtain eigenvectors k_A and k_B . When k_A and k_B are both real, both complex (iq or $\pi \pm iq$) (where $q > 0$), or one is real and the other is complex, we can obtain BM, IM, and PCM, respectively. If k_A and k_B are both iq , both $\pi \pm iq$, or $k_A = iq$ and $k_B = \pi \pm iq$, or $k_A = \pi \pm iq$ and $k_B = iq$, we call the eigenmode, respectively, as the acoustic type interface mode (AIM), the optic type interface mode (OIM), the acoustic type interface mode inside the gap (GAIM), and the optic type interface mode inside the gap (GOIM). Here, the classification of the IMs is in agreement with the result of Ref. 17, i.e., IM is acoustic when the direction of spin oscillation in the interface of sublayer A is the same as that in the adjacent sublayer B , whereas it is optic when the two are opposite. In order to differentiate two different AIMs or two different OIMs possibly existing in the system, however, we only call the acoustic type IM below the energy band AIM

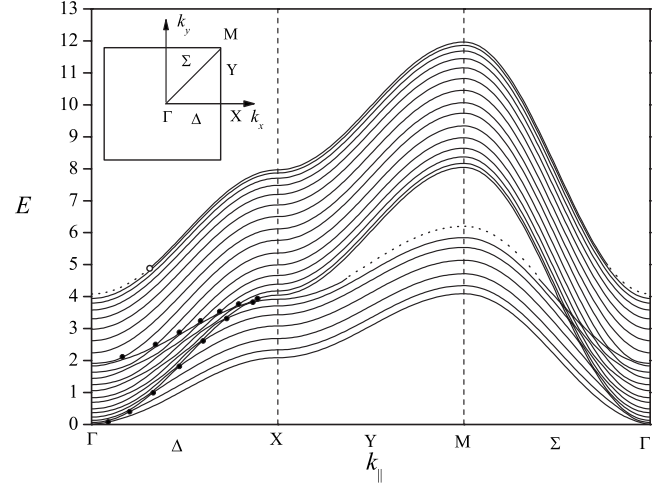


FIG. 1. The energy band mapping (EBM) of 2D Brillouin zone of the bilayer system corresponding to $J_A, J_B, J_{AB}, S_A, S_B, N_A,$ and N_B are, respectively, 1.0, 1.0, 2.0, 1, 1/2, 31, and 15: the higher energy band is subband A , the lower energy band is the subband B , the highest dotted lines denote the OIM, and the dotted line inside the gap denotes the GOIM. The 2D Brillouin zone of the bilayered system is plotted at the top left corner of the EBM, where Δ line, Y line, and Σ line are three high-symmetry paths. The open circle denotes the critical point between OIM and PCMA and full circles denote the critical points between PCMs and BMs on the Δ region of EBM.

and call the optic type IM above the energy band OIM, while the acoustic type IM and the optic type IM inside the gap of the energy band are called, respectively, as GAIM and GOIM as stated above (see Figs. 1 and 8).

III. RESULTS AND DISCUSSION

We analyze in this section the energy band configuration of the longitudinal spin waves with transverse wave vector k_{\parallel} varying along the high-symmetry directions of two-dimensional (2D) Brillouin zone (see Fig. 1). In this model, with isotropic nearest-neighbor exchange interaction, the energy band only consists of BMs and IMs when $J_A S_A = J_B S_B$,²² and furthermore, BMs and IMs are independent of each other whether $S_A = S_B$ or $S_A \neq S_B$; namely, there is no critical position between BMs and IMs, whereas the CMs only exist in the critical positions between different types of eigenmode. So the CMs cannot appear in the system when $J_A S_A = J_B S_B$. Thus, we only discuss the case of $J_A S_A \neq J_B S_B$.

First, we discuss the case that the interface coupling constant J_{AB} is positive. Without any loss of the generality, we assume $J_A S_A > J_B S_B$ and choose the value of the parameter $J_A, J_B, J_{AB}, S_A, S_B, N_A,$ and N_B as, respectively, 1.0, 1.0, 2.0, 1, 1/2, 31, and 15. The numerical results show that the total number of spin-wave modes of the system is 46 ($=N_A + N_B$). For $k_{\parallel} = 0$, the number of BMs is 30 in which there are 14 odd parity modes and 16 even parity modes. The number of PCMs in sublayer A (PCMA) is 14, among which the odd and even parity modes are 50:50. The total number of OIM is

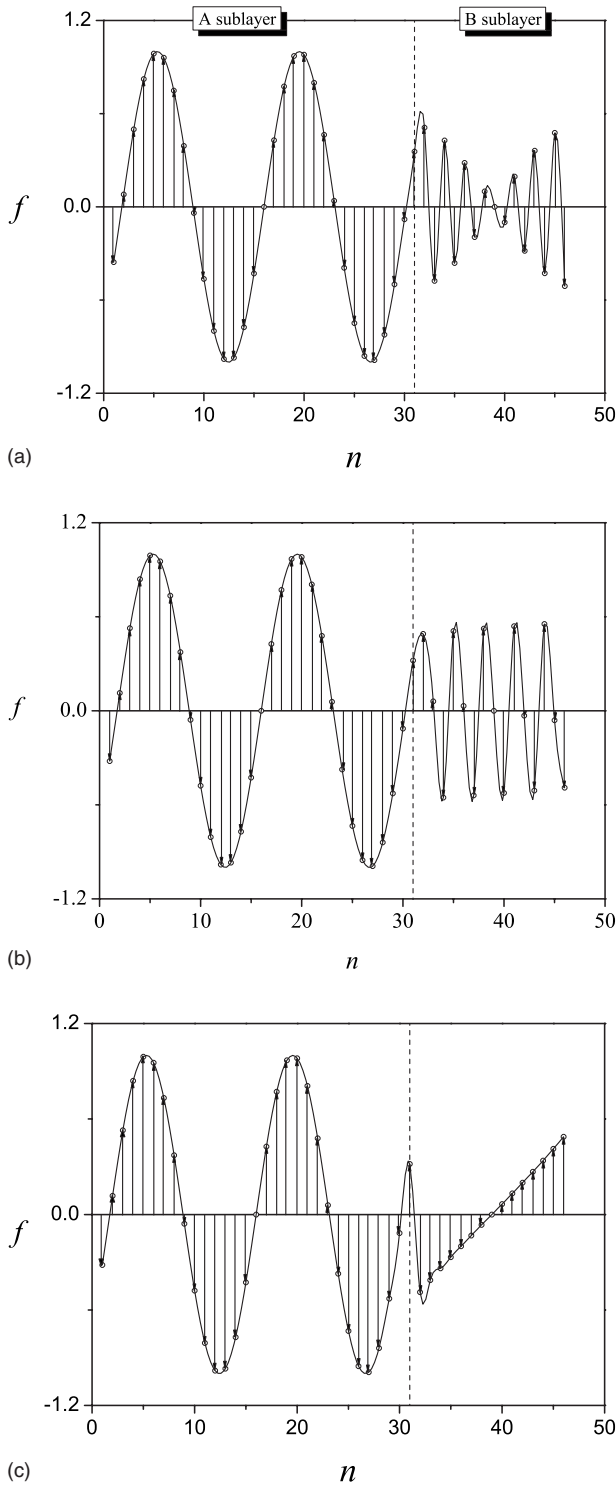


FIG. 2. Wave forms of the ninth eigenmode on the Δ region of 2D Brillouin zone $J_{AB}=2.0$: (a), (b), and (c) are, respectively, SWM of CM at the critical point, the bulk spin wave in front of the critical point, and the spin wave of PCMA behind the critical point, where the arrow denotes the spin vector in every lattice.

2 with different parities. Because the energy band of the even parity modes is similar to the odd parity modes, only the fine structure of the energy band of the odd parity modes is plotted with varying \tilde{k}_{\parallel} along the high-symmetry paths of 2D

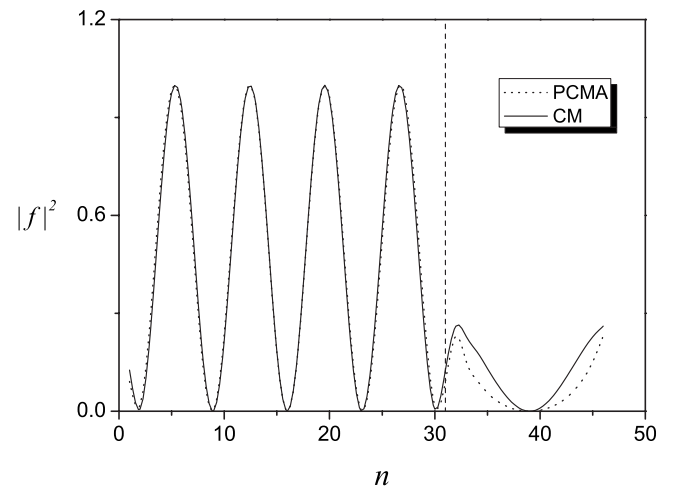


FIG. 3. Wave forms of the amplitude square of the ninth eigenmode on the Δ region of 2D Brillouin zone $J_{AB}=2.0$: the dotted line denotes the spin wave of PCMA and the solid line denotes SWM of CM.

Brillouin zone in Fig. 1. The higher subband consists of PCMA, the lower subband is composed of PCMs in sublayer B (PCMB), and the overlap of the subbands consists of BMs. The highest branch (dotted line) is OIM, and the branch (dotted line segment) within the gap is GOIM. BMs are all standing waves that can freely propagate both in sublayers A and B. PCMs are standing waves in own sublayer, while in the other sublayer, they are surface decaying waves that can only exist on the interface. IMs are surface decaying waves in both sublayers. The open circle denotes the critical point between OIM and PCMA, and full circles denote the critical points between PCMs and BMs on the Δ region of 2D Brillouin zone. At these critical points, we find the critical modes, which are composed of the spin waves modulated by the interface [see Fig. 2(a)]. Wave forms of the ninth eigen-

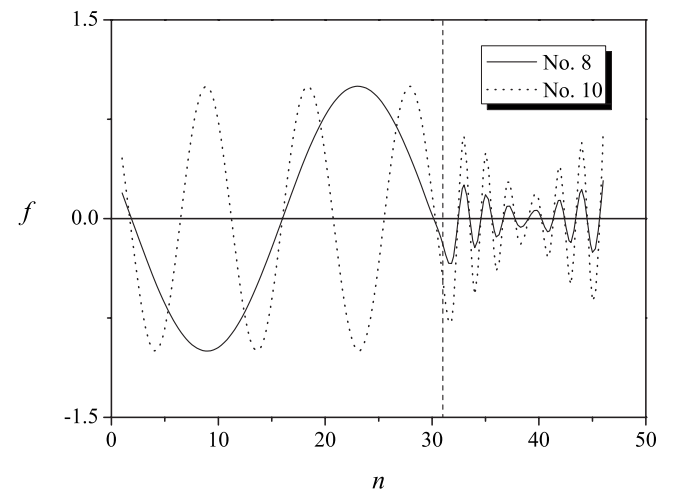


FIG. 4. Wave forms on the Δ region of 2D Brillouin zone $J_{AB}=2.0$: the solid line and the dotted line denote, respectively, SWM of eighth mode at the critical point and SWM of the tenth mode at the critical point.

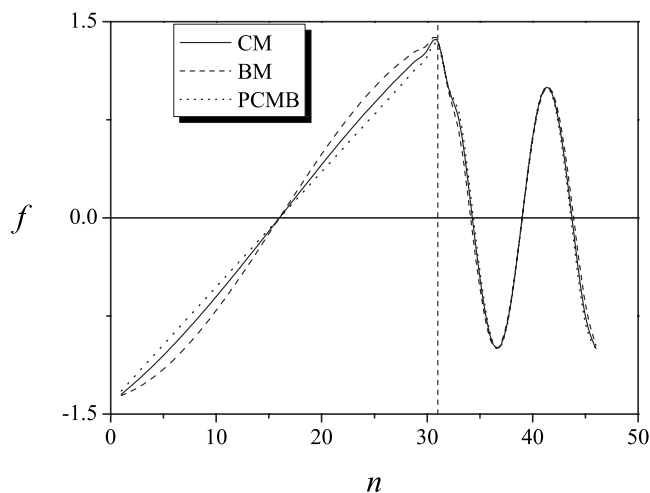


FIG. 5. Wave forms of the second eigenmode on the Δ region of 2D Brillouin zone $J_{AB}=2.0$: the solid line denotes SWM of CM at the critical point, the dashed line denotes the spin wave of BM in front of the critical point, and the dotted line denotes the spin wave of PCMB behind the critical point.

mode on the Δ region of 2D Brillouin zone are plotted in Fig. 2, where the arrow denotes the spin vector in every lattice. Figure 2(a) is SWM corresponding to CM at the critical point $k_x=2.48$, where the modulation appears in sublayer B. Figure 2(b) is the standing wave corresponding to BM in front of the critical point $k_x < 2.48$. Figure 2(c) is the standing wave in sublayer A and the surface delaying wave in sublayer B corresponding to PCMA behind the critical point $k_x > 2.48$. It can be seen that the CM spin wave in sublayer B possesses both the oscillation feature of the bulk spin wave and the decaying feature of the interface spin wave. Apparently, the bulk spin wave in sublayer B is modulated by the interface spin wave in sublayer B to form SWM of CM in sublayer B. So the amplitude square of SWM in sublayer B tends to that of the interface spin wave (see Fig. 3). SWMs in sublayer B exist at all the critical points between PCMA and BMs. As shown in Fig. 4, SWMs in sublayer B of the eighth mode and the tenth mode are plotted. At all the critical points between PCMBs and BMs, the modulation behavior of CM appears in sublayer A. Wave forms of the second eigenmode on the Δ region of 2D Brillouin zone are plotted in Fig. 5, where the solid line denotes SWM of CM at the critical point, the dashed line denotes the spin wave of BM in front of the critical point, and the dotted line denotes the spin wave of PCMB behind the critical point. Figure 5 shows the modulation appears in sublayer A, and SWM tends to the spin wave of PCMB. Similarly, SWM exists at the critical points between IM and PCM. Wave forms of the 22nd eigenmode on the Δ region of 2D Brillouin zone are plotted in Fig. 6, where the solid line denotes SWM of CM at the critical point, the dotted line denotes the spin wave of OIM in front of the critical point, and the modulation appears in sublayer A. At the critical points of the other region of 2D Brillouin zone, SWMs universally exist too. For example, wave forms of the seventh eigenmode on the Y region of 2D Brillouin zone are plotted in Fig. 7, where the solid line denotes SWM of CM at the critical point, the dotted line denotes the spin

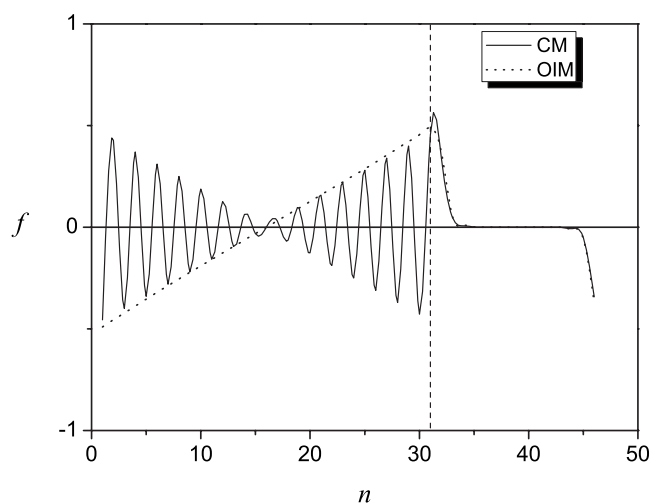


FIG. 6. Wave forms of the 22nd eigenmode on the Δ region of 2D Brillouin zone $J_{AB}=2.0$: the solid line denotes SWM of CM at the critical point and the dotted line denotes the spin wave of OIM in front of the critical point.

wave of GOIM behind the critical point, and the modulation appears in sublayer B.

When the interaction coupling constant J_{AB} is negative, the energy band of this system is plotted in Fig. 8. In this figure, choosing J_{AB} as -0.2 and the other parameters being same as Fig. 1, we find a branch of AIM appears below the energy band and the OIM above disappears. In order to compare with the case of $J_{AB}=2.0$, we label the AIM as No. 0 eigenmode. The CMs still exist at the critical points (the open and full points in Fig. 8) in the system. However, the amplitude of the SWMs (see Fig. 9) is obviously smaller than the one's when $J_{AB}=2.0$ (see Figs. 2 and 4). At the same time, the positions where the CMs exist also have a slight variation. Take example for No. 9 eigenmode. In the position of $k_x=2.48$, the CM exists when $J_{AB}=2.0$, whereas it exists in

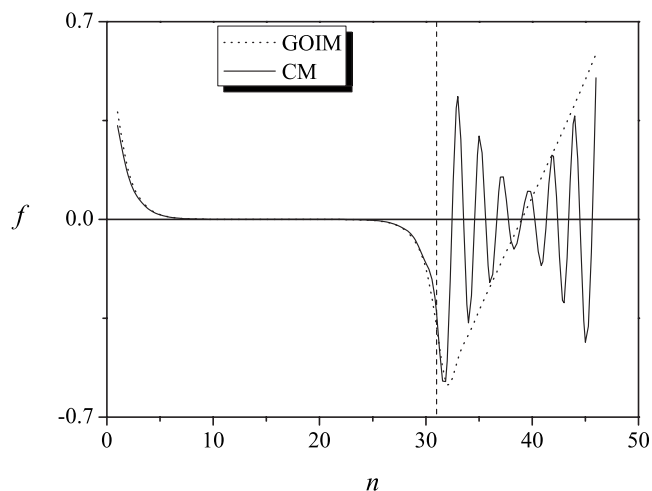


FIG. 7. Wave forms of the seventh eigenmode on the Y region of 2D Brillouin zone $J_{AB}=2.0$: the solid line denotes SWM of CM at the critical point and the dotted line denotes the spin wave of GOIM behind the critical point.

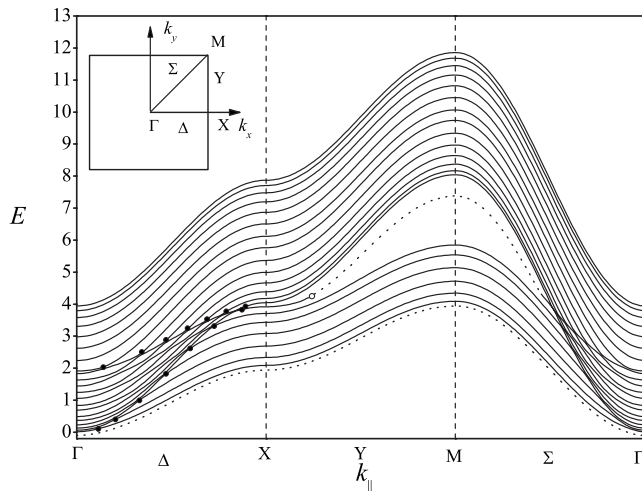


FIG. 8. The EBM of 2D Brillouin zone corresponding to $J_{AB} = -0.2$ and the other parameters are same as Fig. 1. The open circle denotes the critical point between GOIM and PCMB and full circles denote the critical points between PCMs and BMs.

the position of $k_x = 2.40$ when $J_{AB} = -0.2$. This shows the CMs still exist for negative J_{AB} , but the amplitude of the SWMs and the critical position of the CMs change.

At every critical point of 2D Brillouin zone, SWMs exist whether the interaction coupling constant J_{AB} is positive or negative. So the modulation phenomenon is only related to the position of k space and is not related to the mechanism to generate the wave. We conjecture the phenomenon not only appears in the spin wave, but also appears in the lattice wave.

IV. CONCLUSIONS

In summary, we give the energy band fine structure of a general ferromagnetic bilayer system over the whole 2D Brillouin zone. Note that CMs are found at the critical point between BM and PCM or PCM and IM in the system. CM is

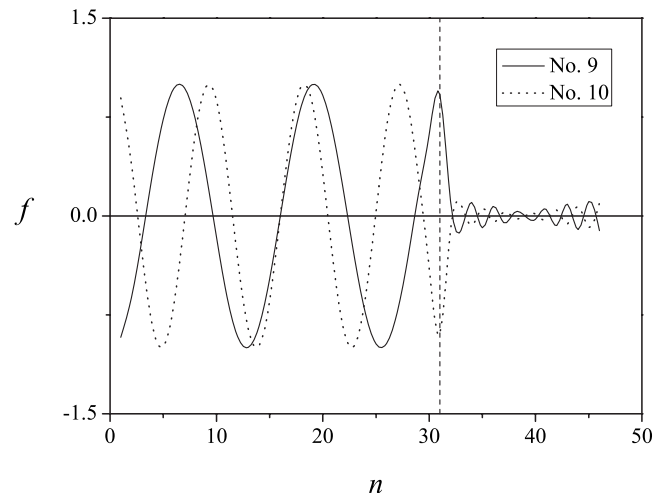


FIG. 9. Wave forms on the Δ region of 2D Brillouin zone for $J_{AB} = -0.2$: the solid line and the dotted line denote, respectively, SWM of ninth mode at the critical point and SWM of the tenth mode at the critical point.

composed of the spin waves modulated by the interface, which possess both the feature of the bulk spin waves and that of the interface spin waves. This result shows that there may be some interesting spin eigenmodes in the magnetic multilayer system. Yet, the spin excitation mentioned above has not been found in the known experiment. So we hope our calculation will stimulate further experimental study.

ACKNOWLEDGMENTS

This work was supported by the Key Project of Chinese Ministry of Education under Grant No. 206024, National Natural Science Foundation of China under Grant No. 10762001, NCET under Grant No. 05-0272, PhD Progress Foundation of higher education institutions of China under Grant No. 20040126003, and Inner Mongolia Natural Science Foundation under Grant No. 200711020109.

*Corresponding author. wenpingzhou73@yahoo.com.cn

¹M. N. Baibich, J. M. Broto, A. Fert, F. Nguyen Van Dau, F. Petroff, P. Etienne, G. Creuzet, A. Friederich, and J. Chazelas, *Phys. Rev. Lett.* **61**, 2472 (1988).

²Uwe Hartmann, *Magnetic Multilayers and Giant Magnetoresistance* (Springer, Berlin, 1999).

³D. J. Monsma, J. C. Lodder, Th. J. A. Popma, and B. Dieny, *Phys. Rev. Lett.* **74**, 5260 (1995).

⁴C. Tsang, R. E. Fontana, T. Lin, D. E. Heim, V. S. Speriosu, B. A. Gurney, and M. L. Williams, *IEEE Trans. Magn.* **30**, 3081 (1994).

⁵E. Y. Chen, S. Tehrani, T. Zhu, M. Durlam, and H. Goronkin, *J. Appl. Phys.* **81**, 3992 (1997).

⁶S. Tehrani, J. M. Slaughter, M. Deherrera, B. N. Engel, N. D. Rizzo, J. Salter, M. Durlam, R. W. Dave, J. Janesky, B. Butcher, K. Smith, and G. Grynkwich, *Proc. IEEE* **91**, 703 (2003).

⁷D. Smith, C. E. S. Khizroev, and D. Litvinov, *J. Appl. Phys.* **99**, 014503 (2006).

⁸S. A. Wolf, D. D. Awschalom, R. A. Buhrman, J. M. Daughton, S. von Molnár, M. L. Roukes, A. Y. Chtchelkanova, and D. M. Treger, *Science* **294**, 1488 (2002).

⁹C. H. Back, R. Allenspach, W. Weber, S. S. P. Parkin, D. Weller, E. L. Garwin, and H. C. Siegmann, *Science* **285**, 864 (1999).

¹⁰J. A. C. Bland, A. D. Johnson, H. J. Lauter, R. D. Bateson, S. J. Blundell, C. Shackleton, and J. Penfold, *J. Magn. Magn. Mater.* **93**, 513 (1991).

¹¹K. Perzlmaier, M. Buess, C. H. Back, V. E. Demidov, B. Hillbrands, and S. O. Demokritov, *Phys. Rev. Lett.* **94**, 057202 (2005).

¹²W. L. Johnson, S. A. Kim, S. E. Russek, and P. Kabos, *Appl. Phys. Lett.* **86**, 102507 (2005).

¹³V. E. Demidov, U.-F. Hansen, O. Dzyapko, N. Koulev, S. O.

- Demokritov, and A. N. Slavin, Phys. Rev. B **74**, 092407 (2006).
- ¹⁴G. Gubbiotti, G. Carlotti, T. Ono, and Y. Roussigne, J. Appl. Phys. **100**, 023906 (2006).
- ¹⁵P. Grunberg, R. Schreiber, Y. Pang, M. B. Brodsky, and H. Sowers, Phys. Rev. Lett. **57**, 2442 (1986).
- ¹⁶R. W. Wang and D. L. Mills, Phys. Rev. B **50**, 3931 (1994).
- ¹⁷R. Zivieri, L. Giovannini, and F. Nizzoli, Phys. Rev. B **62**, 14950 (2000).
- ¹⁸A. Yaniv, Phys. Rev. B **28**, 402 (1983).
- ¹⁹H. Puzskarski and L. Dobrzynski, Phys. Rev. B **39**, 1819 (1989); **39**, 1825 (1989).
- ²⁰G. H. Yun, J. H. Yan, S. L. Ban, and X. X. Liang, Surf. Sci. **318**, 177 (1994).
- ²¹X. X. Liang, X. Wang, S. L. Ban, R. S. Zheng, J. H. Yan, and G. H. Yun, *Theories of the Electron-Phonon Interaction and Spin-Waves in Layered Materials* (Inner Mongolia University Press, Hohhot, 1995) Chap. 5.
- ²²H. Puzskarski, A. Akjouj, B. Djafari-Rouhani, and L. Dobrzynski, Phys. Rev. B **51**, 16008 (1995).
- ²³P. Henelius, P. Fröbrich, P. J. Kuntz, C. Timm, and P. J. Jensen, Phys. Rev. B **66**, 094407 (2002).
- ²⁴G. H. Yun and X. X. Liang, Eur. Phys. J. D **35**, 261 (2003).
- ²⁵M. Krawczyk, H. Puzskarski, J.-C. S. Lévy, S. Mamica, and D. Mercier, J. Phys.: Condens. Matter **15**, 2449 (2003).
- ²⁶W. P. Zhou and G. H. Yun, Surf. Sci. **553**, 75 (2004).
- ²⁷G. Leaf, H. Kaper, M. Yan, V. Novosad, P. Vavassori, R. E. Camley, and M. Grimsditch, Phys. Rev. Lett. **96**, 017201 (2006).